Manipulation of superconductivity in van der Waals materials and thin films

Chen, X.

1

INTRODUCTION

1.1. GENERAL MOTIVATION

Often in life, the most inspiring or exhilarating narratives occur when there is a drastic change over the background of a continuously evolving environment. An earthquake which unexpectedly changes the fate of many ordinary people; the emergence of the butterfly from its chrysalis. In physics, this is frequently also the case. Whether it is the change of the state of matter, such as when water becoming vapour at 100 °C [1] [2]; the quench of the mechanical structure of a crystal at high pressure or temperature [3] [4] [5]; or abrupt changes of magnetic properties and symmetry for a material at a critical temperature [6]. Many popular research topics in modern (condensed matter) physics are carried out on the border of those sudden changes, commonly referred to as phase transitions. Among those, one of the phase transitions has triggered interest from both the theoretical and experimental side. That is the phenomenon of superconductivity.

Superconductivity refers to the sudden vanishing of electrical resistance in a material occurring when certain criteria have been met. In this state of matter, all conducting electrons are allowed to be in the ground state simultaneously through a pairing mechanism. The charge carriers are now comparable to the atoms in a superfluid, where they should be considered as bosons rather than fermions. In this phase, the scattering or defect centres no longer have bearing over the current flow, and the charges move without any dissipation of energy. The concept was so strange and fully quantum that it was never considered in theoretical physics before it was first discovered in the Leiden cryogenic laboratory by Heike Kamerlingh Onnes in 1911 [7].

Ever since this was first discovered, superconductivity has become a crucial part of research topics in condensed matter physics. Phonon-mediated conventional superconductors provide a large platform to study collective bosonic particle interaction with electric and/or magnetic field for generating non-equilibrium quasi-particle states [8] [9] [10]. The study into unconventional and high-Tc superconductors contributes to the progress of understanding strongly correlated electron systems [11] [12]. Designing and engineering topological superconductors by manipulating the surface state has drawn growing attention from both the theoretical and experimental physics communities [13] [14]. More recently, artificial superconductors made by twisting and stacking van der Waals materials opened new doors in understanding and manipulating boundary conditions in quantum materials [15].

On the application side, superconducting quantum interference devices, play a major role in the recent progress in quantum computing [16]. Junction devices which combine superconductivity with magnetism bring opportunities for developing new and more efficient memristors [17]. Superconducting cables and wires have been involved in constructing large research infrastructures [18] [19], especially in building strong magnets for particle physics research facilities [20]. On the nano and micro scale, superconducting wires and strips provide multiple ways of detecting single photos of a wide wavelength spectrum [21]. For those reasons, after more than 100 years since it was first observed, the study and curiosity into superconductivity have only seen growth.

Recently, the field of superconductivity is becoming more and more advanced accompanied by the progress obtained in fields such as material interface science and nanofabrication. Along with the exotic superconductors draw increasing amounts of attention, the conventional phonon-mediated s-wave superconductors are also being explored more and more in different fabrication and measurement techniques. This brings further insight into physics around the phase transition as well as the important role boundary conditions impose on a system.

Being one of the most studied categories of superconductors, there is an immense amount of literature on the topic of conventional superconductors. It is also the most frequently used type of material so far in the application of superconductivity. This thesis belongs to the general effort in studying and understanding the transport properties of those superconductors. Especially thanks to the progress in material fabrication, the possibility of growing new synthetic materials and manipulating their properties becomes available. Therefore bringing new prospects for further development in the field.

This is especially beneficial in the field of thin film and (intrinsic or artificial) van der Waals superconductors, where both types of materials bear potential for unexplored physics in lower dimensions. Here, in this thesis, we will focus mainly on the direction of altering their superconducting properties via careful design of devices. By performing charge transport experiments on our superconducting devices, we carefully explore how the macroscopic properties of the devices can be transformed through deliberate sample manipulations.

1.2. SUPERCONDUCTIVITY

Superconductivity refers to the phenomenon of current flowing without resistance after the system goes through a phase transition. It is well known that in the superconducting phase, the current is carried by pairs of electrons, the so-called Cooper pairs. The paired electrons can be treated as bosonic particles contrary to fermionic electrons. The bosonic Cooper pairs can condense into a single ground state similar to a Bose-Einstein condensate in a superfluid. Unlike a hypothetically perfect conductor, in this bosonic state (below the lower critical magnetic field for type-II superconductor), the magnetic field is completely expelled from the bulk of the solid superconductor. This is known as the Meissner effect.

Several different approaches describe superconductivity theoretically. Here, we will

focus on the Ginzburg-Landau formulation. It is a phenomenological quantum theory that treats the superconducting transition as a second-order phase transition as a function of free energy.

The electrons that are part of the Bose-Einstein condensate can be described macroscopically by a single, complex-valued wavefunction Ψ in terms of the density of Cooper pairs $n_s(\boldsymbol{r}, t)$ and a phase θ:

$$\Psi(\boldsymbol{r}, t) = \sqrt{n_s(\boldsymbol{r}, t)} e^{i\theta(\boldsymbol{r}, t)} \tag{1.1}$$

This is also the order parameter of the phase transition, and the expectation value of it is the density of Cooper pairs. Under an external electromagnetic field, the current density can be derived to be:

$$J = -\frac{(2e)^2 n_s}{m}\left(\boldsymbol{A} + \frac{\hbar}{2e}\nabla\theta\right) \tag{1.2}$$

where $\boldsymbol{A}$ is a magnetic vector potential and m is the mass of the charge carriers. After rearranging and introducing in magnetic flux quantum $\Phi_0 = h/2e$, the Ginzburg-Landau equation for superconducting current density is arrived:

$$J = -\frac{\Phi_0}{2\pi\mu_0\lambda^2}\left(\frac{2\pi}{\Phi_0}\boldsymbol{A} + \nabla\theta\right) \tag{1.3}$$

where $\lambda = \sqrt{m/4\mu_0 n_s e^2}$ is the London penetration depth. Because J is gauge-invariant while $\boldsymbol{A}$ and θ are not; the term between the brackets in equation 1.3 must be gauge-invariant. Now it becomes clear that the supercurrent density is dependent only on parameters that come directly from quantum mechanics. Therefore, superconductivity is a purely quantum phenomenon.

If we take Ψ as purely an order parameter and start from the system's free energy point of view, the other Ginzburg-Landau equation can be derived. This equation describes superconductivity without an external magnetic field, and it is given by:

$$-\xi^2\nabla^2\psi - \psi + \psi|\psi|^2 = 0 \tag{1.4}$$

where $\psi = \Psi(\boldsymbol{r})/\Psi_0$ is a dimensionless wavefunction, and $\xi = \sqrt{\hbar^2/2m|\alpha(T)|}$ is the coherence length. The temperature dependent Ginzburg-Landau parameter $\alpha(T)$ can be introduced as $\alpha_0(T - T_c)$.

We have now introduced two significant characteristic length scales in superconductors; the penetration depth λ and the coherence length ξ. The penetration depth describes the length scale over which an external magnetic field can penetrate into the superconductor. The coherence length describes the minimum length scale over which the superconducting wave function can vary coherently and defines a length scale at which the electrons in the Cooper pairs can be correlated.

The ratio $\kappa = \lambda/\xi$ of the two values is an intrinsic property of the material and it is independent of temperature. It describes to what extent the superconductivity and magnetic field can coexist. For bulk type I superconductors, the value of κ is small $(\kappa < 1/\sqrt{2})$. This indicates the magnetic field lines decay very quickly into the surface

of the bulk superconductor. Thus, a complete Meissner effect always occurs anywhere below the critical magnetic field. For type II superconductors, the value of κ is larger than $1/\sqrt{2}$. This means that, in this type of superconductor, the magnetic field lines can coexist with superconductivity even in bulk materials, in the form of vortices.

1.3. MAGNETIC VORTICES IN THIN FILM SUPERCONDUCTORS

As previously mentioned, for type II superconductors, under an external magnetic field that is higher than its lower critical field, there exists a mixed state where it is energetically more favourable to have the coexistence of superconducting and normal domains where the magnetic flux can locally penetrate the superconductor. Those individual normal domains are called vortices, and they each can sustain a magnetic flux of one flux quantum Φ_0. The radius of the normal domain is of order coherence length ξ. Outside the normal domain, at a radius of about penetration depth λ, runs a circulating supercurrent to generate a magnetic field in the same direction as the external magnetic field. The scales of ξ, λ and the geometry of the system play a large role in how the vortices interact and move in the superconductor.

In this thesis, we primarily focus on superconducting samples that are suppressed in one dimension compared to the other two. We define thin film superconductors as superconductors whose thickness is comparable to or smaller than the coherence length. In such cases, the surface energy has a dominant effect on the overall behaviour of the system. Moreover, the reduced dimension often has a strong influence on both the electronic density of states [22] and electron-phonon coupling [23] [24]. Thus, the properties observed in thin film superconductors are often very different from their bulk form. For example, most thin film type I superconductors can be effectively treated as type II superconductors due to the dominant effect of the stray magnetic field.

An important parameter in the discussion concerning thin film superconductors under an external magnetic field is the Pearl length. Due to the major role played by the surface energy, field lines that penetrate thin superconductors behave differently than that of bulk samples, especially near the superconductor to vacuum interface [25]. The field lines will have broader and broader distributions with decreasing thickness. This needs to be accounted for when considering interactions between vortices. The Pearl length can be calculated by:

$$\Lambda = \frac{2\lambda(0)}{d}\lambda(0) = \frac{2\lambda(0)^2}{d} \tag{1.5}$$

where d is the film thickness, and $\lambda(0)$ is the London penetration depth at $T = 0K$. The Pearl length describes the characteristic length of the distribution of the magnetic flux lines for each vortex.

If the Pearl length is much larger than the London penetration depth and the film thickness but comparable to the width of the device size $(\lambda(0)/d \gg 1)$, the vortices interact in the superconductor as the Pearl vortex. In this case, the interaction potential between

vortices can be approximately expressed as follows [26]:

$$V(r) \approx \frac{\Phi^2}{2\pi\Lambda\mu_0} \ln\left(\frac{2.27\Lambda}{r} - \frac{0.27\Lambda}{9\Lambda + r} + 1\right) \tag{1.6}$$

which shows a $ln(1/r)$ dependence at short distance and $1/r$ dependence at larger distance.

When the Pearl length is much larger than both the coherence length and the width of the device size, the vortices form Abrikosov lattices on the superconducting film, just as in the bulk superconductor [27]. In this case, the vortex formation can be directly derived from the Ginzburg-Landau theory. The field strength for each vortex falls off exponentially from the vortex core. Minimising the free energy of the system, it can be shown that the vortices arrange themselves to form a favourable triangular lattice with a lattice constant in the order of λ. When the external magnetic field is increased to the extent that the lattice constant becomes of the order of ξ, the normal area of the vortices starts to overlap, and the superconductivity across the whole sample disappears. The field strength where this happens is known as the upper critical field.

When there is a supercurrent running in the superconductor, the vortices will experience a Lorentz force generated by the combination of magnetic field and the current. Assuming there is no opposing pinning force, the vortices flow across the supercurrent only damped by their viscosity, also known as flux flow. This viscous flow dissipates energy which and gives a flow resistivity ρ_f. Equating the viscous force to the Lorentz driving force $J\Phi_0 = \eta v$ and substituting $E = Bv$, we find:

$$\rho_f = \frac{E}{J} = \frac{B\Phi_0}{\eta} \tag{1.7}$$

where η is the viscous drag coefficient. The flow resistivity is proportional to the magnetic field and inversely proportional to the viscous drag coefficient.

Now let us pay more attention to the velocity of the moving vortices. Assuming the external magnetic field is fixed to a value between the lower and upper critical field, an increase in the injection current will exert a larger Lorentz driving force on each vortex. Experimentally, the systems almost always diverge from the ideal case, realisable superconductors tend to contain defects, impurities, grain boundaries, or other inhomogeneities that affect the uniformity of surface free energy. Those local variations act as a pinning force on the vortices that oppose the Lorentz force. When the injection current increases beyond the depinning current, the Lorentz force dominates over the pinning force; flux flow starts to dissiupate energy. This is often reflected in the data as a highly non-linear conductance regime outside the zero resistance part of the current-voltage curve (I-V curve). This resistance might appear well below the de-pairing current, which is the maximum current a superconductor can sustain without breaking up its Cooper pairs.

As the vortex continues to move faster, a quench to the normal resistance state of the superconductor will occur due to the escape of quasiparticles from the vortex core. This is known as the flux flow instability, the last low-resistivity point before the jump to the superconductor's normal state in the I-V curve. According to the Larkin-Ovchinnikov

model, this is due to the increase in the electric field generated by vortex motion, which will increase the kinetic energy of the quasiparticles inside the vortex core to the point where they can overcome the potential barrier around the vortex core, and therefore escape [28]. As the core continues to shrink due to the escape of quasiparticles, the vortices experience avalanching acceleration, and the sample jumps to the normal state. Within this framework, the flux flow instability velocity is given by:

$$v_{LO} = \left(\frac{D[14\zeta(3)]^{1/2}(1-t)^{1/2}}{\pi\tau_\varepsilon}\right)^{\frac{1}{2}} \tag{1.8}$$

where the D is quasiparticle diffusion coefficient, $\zeta(x)$ is the Riemann function, $t = T/T_c$ and τ_ε is the quasiparticle energy relaxation time. The model fits well at the higher magnetic fields where the quasiparticles have a non-uniform distribution around each vortex core.

To account for the uniform quasiparticle distribution between vortices at smaller fields, Doettinger et al. later proposed adding a spatial term that included the vortex lattice [29]. The flux flow velocity is, therefore, related to both magnetic field and temperature as follows:

$$v = \left(\frac{D[14\zeta(3)]^{1/2}(1-t)^{1/2}}{\pi\tau_\varepsilon}\right)^{1/2}\left(1+\frac{\sqrt{2\Phi_0 B/\sqrt{3}\mu_0}}{\sqrt{D\tau_\varepsilon}}\right) \tag{1.9}$$

Now it becomes evident that the instability velocity has a $B^{1/2}$ and $(1-T/T_c)^{1/4}$ dependence. This equation is particularly useful, as a fitting of v in either temperature or magnetic field will obtain quasiparticle energy relaxation time as the fitting parameter, which is an important characteristic scale for some applications of thin film superconductors.

It is important to notice the above description works in the ideal case where the pinning force for the vortices does not drastically vary over the whole superconductor. In experiments, the dependency of v on magnetic field or temperature might deviate from the expected tendency. This is often caused by local structural variation or special sample geometry acting as pinning centres that result in a nonuniform vortex flow across the sample. The local pinning centres for vortices not only decrease the flux flow instability velocity during the flux flow, but they also exert a larger pinning force on the vortices to begin with before flux starts to flow. As such, it is a common practice to artificially add defects to increase the critical current density of the superconductor [30] [31] [32].

1.4. VAN DER WAALS SUPERCONDUCTORS

Van der Waals materials refer to layered materials where chemical bonds only exist within the layer, while whereas between the layers there is only the weak van der Waals force keeping them together. This allows ultra-thin single layer samples to be fabricated by exfoliating bulk crystals. The family of van der Waals materials covers a large range of materials, including insulators, semiconductors and intrinsic superconductors. In this thesis, we will only focus on one particular intrinsic van der Waals superconductor; transition metal dichalcogenide $NbSe_2$.

$NbSe_2$ has multiple polytypes. Polytype refers to a (quasi-)stable configuration in which the layers can be stacked together. In $NbSe_2$, the 3R form polytype is a metal whereas the 2H is superconducting. The crystal structure for 2H-$NbSe_2$ is shown in figure 1.1 (a). In bulk form, 2H-$NbSe_2$ has a critical temperature of around 7 K. Just as with other types of superconductors, when approaching the single layer limit, the critical temperature of the sample decreases. Single layer $NbSe_2$ has a reported critical temperature of around 1-2 K, making it one of few van der Waals superconductors that exhibit measurable superconductivity at the monolayer limit. As will be further introduced later in the thesis, even though it is one of the most studied layered superconductors, new potential and opportunities continue to emerge from studying this special system. More discussion on the monolayer $NbSe_2$ system will be continued in Chapter 3.

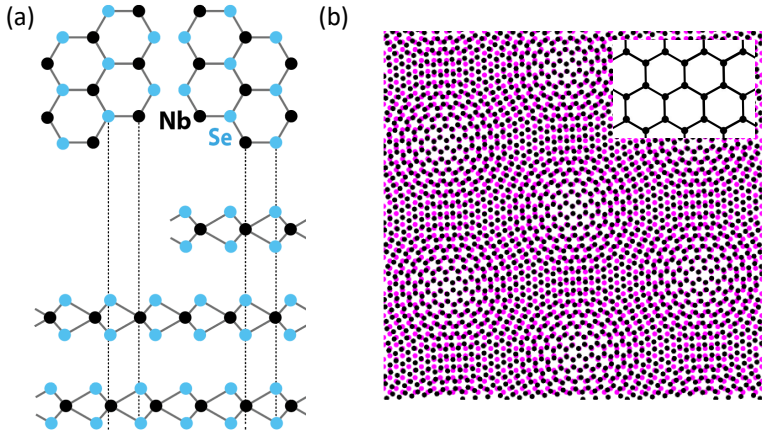

Figure 1.1: Van der Waals materials. (a) Top and side views of the lattice structure of 2H-$NbSe_2$. (b) Moiré pattern of twisted bilayer graphene with 5° twist angle. Insert shows the lattice structure of a single layer graphene.

Apart from the intrinsic superconductors, the simplicity of manipulating van der Waals materials also provides a platform for studying complex quantum devices made by stacking one or multiple van der Waals materials together. They are generally known as heterostructures [33]. Very recently, a unique type of artificial van der Waals superconductor was observed in experiments: superconductivity realised in heterostructures. Of these, the most famous case is the correlated electron system in magic angle twisted bilayer graphene.

When placing two layers of graphene on top of each other with a relative twist angle, a moiré pattern will form due to the misalignment of the two graphene lattice structures. The generated moiré lattices can be orders of magnitude larger than the pristine graphene lattice constant depending on the twist angle. An example of a moiré pattern of two graphene monolayers at a twist angle of 1.1° is shown in figure 1.1 (b). The original hexagonal graphene lattice is shown in the inset. The hybridization of the electronic bands between the two layers as a result of intralayer coupling produces a very different electronic band than the original Dirac cone of monolayer graphene. At a series of discreet angles, the band near the Fermi energy becomes completely flat, decreasing the kinetic energy of the electrons occupying the band. Thereby a strongly correlated electron system

is created. The device can then be fine tuned into the superconducting phase by either the electric doping or magnetic field. Those angles are frequently referred to as magic angles, and they can be calculated by [34][35]:

$$\theta_{mag} = \arccos\Big(\frac{k^2 + 4kl + l^2}{2(k^2 + kl + l^2)}\Big) \tag{1.10}$$

with k, l being integers. The first magic angle can now be calculated with $k = 30$, $l = 31$ to be $1.1°$. Different from the intrinsic van der Waals superconductor, the phase diagram for this artificial superconductor is comparable to that of the cuprate superconductors [36][15].

The same principle has now been extended to and observed in twisted trilayer, quadruple layer and even more graphene layers. Similar phase diagrams have also been observed in twisted transition metal dichalcogenide layers [37]. The stacking order is proven to be a fundamental parameter in modifying the quantum properties of the layered materials. This poses the question of whether the same way of artificial reshaping electronic bands can be extended to other bulk superconductors.

1.5. JOSEPHSON JUNCTIONS

A Josephson junction refers to a device where two superconducting macroscopic wave functions are coupled together through a thin barrier, often known as a weak link. The study of junction physics provide an effective tool to probe directly into the phase relations between two superconductors, especially in terms of symmetry law. It also brings opportunities for directly measuring the effective penetration depth of the superconductor. Moreover, the Josephson junctions are the base for superconducting quantum interference devices (SQUIDs), which are very useful in both measuring micromagnetic field as well as building digital electronic circuits.

A schematic drawing of a Josephson junction is shown in figure 1.2 (a). The supercurrent that can flow through the weak link is related to the phase difference of the two superconducting wave functions:

$$I_s = I_c \sin(\theta_2 - \theta_1) \tag{1.11}$$

where I_c is the maximum amount of supercurrent that can be sustained by the junction.

When the junction is under a magnetic field that is perpendicular to the supercurrent direction, the field flux trapped in the weak link will add an extra phase difference to the two wavefunctions. Therefore, the current passing through the junction as a function of the external magnetic field is:

$$\begin{aligned} I(B) = \int \boldsymbol{J}\, d\boldsymbol{S} &= \int_{-H/2}^{H/2} W J_c \sin\Big(\theta_2 - \theta_1 + \frac{2\pi LB}{\Phi_0} y\Big)\, dy \\ &= \mathrm{Im}\Big[e^{i(\theta_2-\theta_1)} W \int_{-\infty}^{\infty} J_c(y) e^{2\pi i \beta y}\, dy\Big] \end{aligned} \tag{1.12}$$

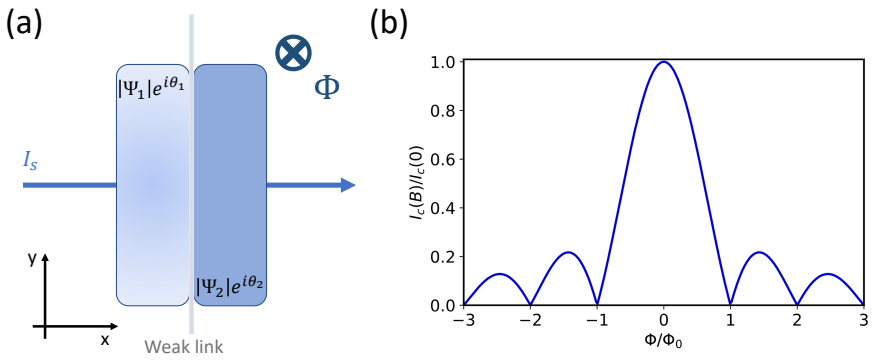

Figure 1.2: (a) A schematic layout of a Josephson junction under a magnetic field in the z-direction, where the two macroscopic wavefunctions are coupled via the weak link. (b) The Fraunhofer interference pattern of the junction's critical current oscillation in units of the flux quantum Φ_0.

Where W (junction size in the z-direction) and H (junction size in the y-direction) are the width and height of the junction, L is the effective junction length $2\lambda + d$; d is the length of the weak link (in the y-direction). In the second part of the equation, we have substituted field B with $\beta = LB/\Phi_0$. The integration bounds can also be extended to infinity as there cannot be physical supercurrent outside the device dimension. As the phase factor $\theta_2 - \theta_1$ has the maximum value at critical current, it can be dropped out of the equation when we are only considering the junction critical current. Therefore, the critical current per unit width is:

$$I_c(B) = \left| \int_{-\infty}^{\infty} J_c(y) e^{2\pi i \beta y} \, dy \right| \tag{1.13}$$

Here, we recognise that junction critical current is simply a Fourier transform of the supercurrent density in the y direction with the boundary being the device geometry. This implies that an inverse Fourier transform of the critical current in the magnetic field will yield the distribution of supercurrent density in the y direction.

For a junction with uniform supercurrent density along the y direction within the device, by substituting the maximum phase factor $\theta_2 - \theta_1 = \pi/2$ and $B = 0$, we can obtain the following:

$$\frac{I_c(B)}{I_c(0)} = \frac{\sin(\pi\Phi/\Phi_0)}{\pi\Phi/\Phi_0} \tag{1.14}$$

This is plotted in figure 1.2 (b) in the unit of flux quantum Φ_0. As shown, the ideal critical current oscillating with the magnetic field following a pattern that is the Fraunhofer interference pattern well known in optical diffraction experiments as the diffraction pattern of a single-slit. Measuring the interference pattern of Josephson junction critical current in the magnetic field is a great tool to study the superconducting properties of the superconductors. In addition, as previously shown, by Fourier analysing the obtained pattern the geometric effect on the junction behaviour can be obtained.

1

1.6. OUTLINE OF THIS THESIS

The thesis focuses mostly on the transport studies of van der Waals and thin film superconductors. Chapters 3-5 describe general studies on the fabrication and magnetic response of quasi-2D superconductors. Chapters 6-8 attempt to understand artificial superconductivity generated by electronic band manipulation.

- Chapter 2 gives a small introduction to the experimental setup and technique frequently quoted throughout the thesis. The aim is to give the reader a clear understanding of the methods of research that will be described in the later chapters.
- Chapter 3 describes a recently developed technique in mechanical exfoliation of transition metal dichalcogenide: Gold-assisted exfoliation. Ultra-large (mm in diameter) areas of monolayer $NbSe_2$ are obtained by the method. Unfortunately, we did not observe any superconducting phase transition in the monolayer samples down to 1.4 K. This might be due to the proximity effect or the rough surface of the metal substrate.
- Chapter 4 shows a simple model for understanding the shape of oscillation patterns in heterostructure Josephson junctions. The model is developed based on a transport study in the magnetic field of a junction made by stacking two bulk superconducting $NbSe_2$ flakes on top of each other. The calculated interference pattern is in good agreement with our experimental data.
- Chapter 5 reports a drastic change in flux flow instability velocity in thin-film NbRe samples as well as its dependency on the magnetic field caused by the light oxidation of the sample. We propose the possible reason might be that the domain wall between the oxidised patches and clean surface acts as the trapping centre for vortex flow. We expect a similar effect on other air-sensitive polycrystalline thin film superconductors.
- Chapter 6 describes a simple yet effective dry-stamping fabrication method for twisted bilayer graphene tailored for a Low Energy Electron Microscopy study. Moiré patterns of the sample were obtained and analysed along with Atomic Force Microscope measurements on the same sample.
- Chapter 7 attempts to increase the critical temperature of 50 nm thick MgB_2 by imposing a larger periodic potential on the pristine electronic band. With the inspiration taken from van der Waals superconducting heterostructure, a focused ion beam was used to nano-pattern a periodic structure on the device. A detailed transport study shows further experiments are needed to reach a conclusive verdict.
- Chapter 8 presents a transport measurements of graphene with a monolayer of a Co-TCPP network on the surface. The aim of this work is to induce side band opening in graphene through a periodic potential of the molecular network. Although the properties of graphene did vary, unfortunately, no significant evidence of opening of the sideband was found.